Solar Energy Materials & Solar Cells 114 (2013) 82–88

Contents lists available at SciVerse ScienceDirect

Solar Energy Materials & Solar Cells

journal homepage: www.elsevier.com/locate/solmat

Influence of alkanediol series as processing additives in photo-active layer on the power conversion efficiency of polymer solar cells

Soo Won Heo [a], Kwan Wook Song [a], Min Hee Choi [a], Hwan Sool Oh [b], Doo Kyung Moon [a,*]

[a] Department of Materials Chemistry and Engineering, Konkuk University, 1 Hwayang-dong, Gwangjin-gu, Seoul 143-701, Republic of Korea
[b] Department of Electronic Engineering College of Information & Communication, Konkuk University, 1 Hwayang-dong, Gwangjin-gu, Seoul 143-701, Republic of Korea

ARTICLE INFO

Article history:
Received 22 November 2012
Received in revised form
28 January 2013
Accepted 3 February 2013
Available online 27 March 2013

Keywords:
PSCs
Alkanediols
Processing additive
P3HT
Degree of crystallinity

ABSTRACT

The alkanediol series such as 1,2-ethanediol, 1,3-propanediol, 1,4-butanediol, 1,6-hexanediol, 1,8-octanediol and 1,10-decanediol was introduced to poly(3-hexylthiophene, P3HT):[6,6]-phenyl-C_{61}-butyric acid methyl ester (PCBM) based bulk-heterojunction (BHJ) polymer solar cells as processing additives. When 1,3-propanediol was introduced to photo-active layer as a processing additive, power conversion efficiency (PCE) was dramatically increased from 3.5% (for the reference device) to 5.3%. To investigate the causes of improvement of the PCE of PSCs after addition of alkanediol series, photon absorbance properties were observed using UV–vis spectroscopy and photoluminescence (PL). Then, the degree of crystallinity of P3HT was examined through X-ray analysis. In addition, changes in the nano-structure and surface morphology of P3HT:PCBM blend film were observed through AFM and TEM. The series resistance (R_S) of the fabricated PSCs was 5.19 Ω cm^2, and short circuit current density (J_{SC}), open circuit voltage (V_{OC}) and fill factor (*FF*) were 16.2 mA/cm^2, 0.63 V and 51.9% respectively.

© 2013 Elsevier B.V. All rights reserved.

1. Introduction

Thanks to their good stability for thin film formation, good mechanical properties and excellent electro-optical properties, π-conjugated polymers have attracted great attention as next-generation device materials for organic electric devices [1–5]. In polymer solar cells (PSCs), in particular, solution processes such as screen printing [6], ink-jet printing [6], slot die coating [7], roll to roll stamping [8–11] and brush painting method [12,13] are applicable. Therefore, light-weight and flexible large-area photovoltaic devices can be implemented at low costs. Typically, bulk heterojunction (BHJ) PSCs, which are promising device configuration for high power conversion efficiency (PCE), involve the use of a phase-separated blend of an electron-donating material (p-type conjugated polymers) and an electron-accepting material (n-type fullerene derivatives) as the active layer [14,15].

Tremendous efforts have been made to optimize the photo-active layer formation [16] and the device configuration [17,18], as the maximum PCE of the BHJ PSCs are dramatically increased up to about 8–9% [19,20]. To improveme the PCE of BHJ PSCs, it is necessary to properly form continuous pathways to transfer excited electron and hole to the external circuit without leading to their recombination with each other. The typical BHJ PSCs constitute the system which has poly(3-hexylthiophene, P3HT) as an electron donor and [6,6]-phenyl-C_{61}-butyric acid methyl ester (PCBM) as an electron acceptor. In this system, PCBM is dispersed among P3HT chains and prevents P3HT from being crystallized. Therefore, initial BHJ PSCs show 2.8% of PCE [21]. In order to improve the PCE of P3HT/PCBM BHJ PSCs, therefore, P3HT and PCBM should exist in an interpenetrating network form, and they should be phase-separated very well. In several groups, efficiency has been improved by forming a well-defined bicontinuous interpenetrating network between P3HT and PCBM by controlling thermal annealing time and temperature of BHJ films and using various solvents for dissolving P3HT and PCBM [22–30]. Due to these efforts, P3HT based PSCs improved PCE up to ca. 5%.

As an alternative, Zhang et al. introduced 'solvent mixture' method which blended two different solvents in terms of boiling point [31]. Even though P3HT chain was reorganized by introducing the solvent mixture to which a small amount of chlorobenzene (b.p. 132 °C) was added to the host solvent 'chloroform (b.p. 61 °C)', low PCE (2.3%) was observed.

The studies on BHJ PSCs with low-band gap polymers as an electron donor material whose performance was enhanced by adding a few volume percent of processing additives (e.g. 1,8-diiodooctane, 1,8-octanedithiol, etc.) to the host solvent in a similar method have also been reported [32,33]. These processing additives can improve the order in low-band gap polymer blends with PCBM. The improved order was reflected in a higher hole mobility, higher FFs, and a reduced series resistance. However, most known processing additives have been applied to the cases in which low-band gap polymer exist.

* Corresponding author. Tel.: +82 2 450 3498; fax: +82 2 444 0765.
E-mail address: dkmoon@konkuk.ac.kr (D.K. Moon).

0927-0248/$ - see front matter © 2013 Elsevier B.V. All rights reserved.
http://dx.doi.org/10.1016/j.solmat.2013.02.004

In P3HT/PCBM system, alkanethiols (e.g. n-hexylthiol, n-octylthiol or n-dodecylthiol.) were added to P3HT/PCBM blend, and these allowed the formation of thin films with slightly enhanced hole mobility and charge-carrier lifetimes, because of enlarged P3HT domains with higher crystallinity. Nevertheless, some thermal annealing was still necessary to give the highest possible performance [34].

In this study, therefore, PCE of PSCs was dramatically increased through improving the order in P3HT blends with PCBM and photon absorption property of BHJ film by introducing the novel processing additives 'alkanediol series' to the P3HT/PCBM system. Alkanediol series, which was used as a processing additive, has a higher b.p. than the host solvent as 1,2-dichlorobenzene (ODCB, 180 °C). In addition, we found that the alkanediol selectively dissolves PCBM which was well dispersed in alkanediol, but P3HT was not soluble in alkanediol. For this reason, adding alkanediol series to ODCB without any thermal treatment could improve the ordering of the polymer domain. This study has figured out the causes of improvement of the properties of BHJ PSCs by observing the optical, electrical and structural properties of BHJ film after addition of processing additives. Using UV/ PL spectroscopy, the absorption of photon and the quenching properties of excited electron were observed. In addition, the structural properties of P3HT crystalline were analyzed through XRD pattern analysis. Furthermore, phase segregation of P3HT/PCBM film and increase of crystallinity in P3HT were observed through AFM and TEM analyses.

2. Materials and measurements

2.1. Materials

Indium tin oxide (ITO) glass used as the transparent electrode was produced by Samsung Corning (ITO:170 nm, 10 Ω/sq). Poly(3,4-ethylenedioxythiophene)/poly(styrenesulfonate) (PEDOT:PSS, AI 4083) was purchased from Clevios, and P3HT, which was used as a donor material in the photoactive layer, was purchased from Rieke metal. PCBM, the acceptor material, was purchased from Nano C. 1,2-dichlorobenzene (ODCB), used as a host solvent, and 1,2-ethanediol (2-DO), 1,3-propanediol (3-DO), 1,4-butanediol (4-DO), 1,6-haxenediol (6-DO), 1,8-octanediol (8-DO) and 1,10-decanediol (10-DO), used as processing additives, were purchased from Aldrich. The chemical structures of P3HT and PCBM are shown in Fig. 1(a) and (b) respectively. In addition, the chemical structures of alkanediol series are shown in Fig. 1(c).

2.2. Measurements

All of the thin films were fabricated using a GMC2 spin coater (Gensys), and their thicknesses were measured using an alpha step 500 surface profiler (KLA-Tencor). The photon absorption property and the quenching property of the excited electrons in the BHJ film were measured with UV–vis spectroscopy (HP Agilent 8453) and PL spectroscopy (Perkin Elmer LS 55 luminescence spectrometer), respectively. The XRD patterns were observed using a Rigaku D/MAX 2200 diffractometer with Cu Kα radiation to confirm the crystalline size of P3HT. The morphology of the BHJ films was observed through AFM (PSIA XE-100) and FE-TEM (FEI Tecnai G2 F30), respectively. The surface energy was measured with a contact-angle meter (KRUSS K6). The current density–voltage (*J*–*V*) characteristics of the PSCs were measured using a Keithley 2400 source measure unit. The devices were evaluated at 298 K by using a Class A Oriel solar simulator (Oriel 96000 150 W solar simulator) with a xenon lamp that simulates AM 1.5G irradiation (100 mw/cm^2) from 400 to 1100 nm. The instrument was calibrated with a monocrystalline Si diode fitted with a KG5 filter to bring the spectral mismatch to unity. The calibration standard was calibrated by the National Renewable Energy Laboratory (NREL). IPCE (Mc science) was measured against the best-performing device.

3. Experimental part

3.1. Cleaning of patterned ITO glass

To clean the patterned indium tin oxide (ITO) glass, detergent (Alconox® in deionized water, 10%), acetone, isopropyl alcohol and deionized water were each sonicated in order for 20 min. Moisture was removed by blowing thoroughly with N_2 gas. To ensure complete removal of all of the remaining water, the patterned ITO glass was baked on a hot plate for 10 min at 100 °C. For hydrophilic treatment of the patterned ITO glass, it was cleaned for 10 min in a UVO cleaner.

3.2. Fabrication of PSCs

PEDOT:PSS was spin coated from aqueous solution to form a film of thickness of ca. 40 nm on the patterned ITO glass. The substrate was dried for 20 min at 120 °C in air and then transferred into a glovebox for spin coating the active layer. P3HT and PCBM were dissolved in ODCB with 1:0.6 (P3HT:PCBM=10 mg/ml:6 mg/ml) weight ratio. 2-DO, 3-DO, 4-DO and 6-DO were added to the solutions with various concentrations and mixed by a centrifugal mixer (Thinky ARE-310) at 2000 rpm for 10 min in order to make a well dispersed solution. 8-DO and 10-DO, which are white solid, were insoluble in ODCB; the mixture solution was subjected to thermal treatment by hot plate at 100 °C for 1 h. Then, mixture solution, in which processing additives as 8-DO and 10-DO were added, was mixed by a centrifugal mixer at 2000 rpm for 10 min. The blend solution was then spin coated on top of the PEDOT:PSS layer. The thickness

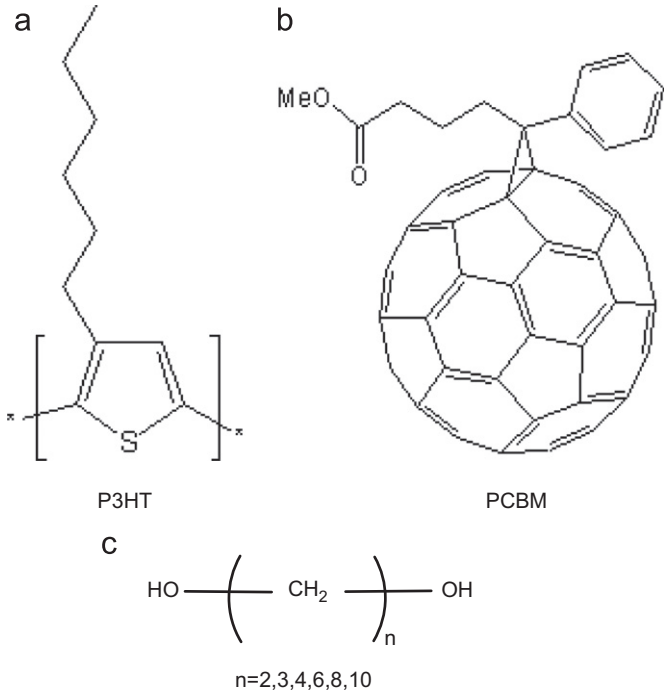

Fig. 1. The chemical structures of (a) P3HT, (b) PCBM and (c) alkanediol series as processing additives.

of photoactive layer was ca. 130 nm and then its vacuum treatment was done at 1×10^{-6} Torr for 60 min. To form the cathode, BaF_2 (0.1 Å/s, 2 nm), Ba (0.2 Å/s, 2 nm) and Al (5 Å/s, 100 nm) were thermally deposited in order in a high-vacuum chamber. Finally, PSCs with an active area of 4 mm^2 (2 mm × 2 mm) were fabricated through encapsulation.

4. Results and discussion

In terms of configuration, PSCs were structured with ITO/PEDOT:PSS/P3HT:PCBM:alkanediol series/BaF_2/Ba/Al, various concentrations of alkanediol series (ODCB/alkanediol series: 99–99.5/0.5–1.0 vol%), and were then characterized without thermal annealing.

The photovoltaic properties of the PSCs with various concentrations of alkanediol series are summarized in Table 1. Fig. 2 shows *J–V* curve and external quantum efficiency (EQE) when alkanediol series was added as a processing additive. The optimized concentration of the processing additive was 0.7 vol% and the vacuum treatment time was 60 min (Figs. S1 and S2). When 3-DO was added as a processing additive, open circuit voltage (V_{OC}), short circuit current density (J_{SC}) and fill factor (*FF*) were 0.63 V, 16.2 mA/cm^2 and 51.9%, respectively. Theoretical J_{SC} values calculated by integrating the product of EQE with the AM 1.5 solar spectrum agree with the measured value with 5%. In other words, the calculated PCE was 5.3%, increased by 52% compared to the reference. Here, the EQE maximum value was 63% at 550 nm. In addition, the devices to which 2-DO, 4-DO and 6-DO were added were 4.9%, 5.1% and 4.9% respectively in terms of PCE. However, the PCE to which 8-DO and 10-DO were added was 3.1% and 2.8% respectively which were slightly less efficient than the reference. In the devices whose efficiency has improved with the addition of processing additive, J_{SC} was dramatically improved, compared to the reference. To investigate the causes of these results, series resistance (R_S) was measured in each device (Table 1). When 3-DO was added, R_S was 5.19 Ω cm^2, decreased by about 42% compared to the reference (7.38 Ω cm^2). The R_S of the device decreased by adding 3-DO, which indicate that the mobility of the charge carriers increases [26]. Therefore, J_{SC} was increased in accordance with the R_S decrease. These patterns were also observed in the devices to which 2-DO, 4-DO and 6-DO were added because the four different processing additives which were added to the photoactive layer changed their nano-structure and surface morphology.

Fig. 3 shows the photon absorption properties with an addition of processing additives, which was observed using UV–vis spectroscopy. Fig. 3(a) shows the UV–vis spectrum of the device in which processing additives (0.7 vol%) were added to the P3HT film. It has been confirmed that when 2-DO, 3-DO, 4-DO and 6-DO were added, the device was better than P3HT in terms of photon absorption properties. Fig. 3(b) shows the UV–vis spectrum of the device in which alkanediol series (0.7 vol%) was added to the

Table 1
Photovoltaic performances of PSCs composed P3HT:PCBM fabricated with diol series as processing additives.

Additive	J_{SC} [mA/cm^2]	V_{OC} [V]	FF [%]	PCE [%]	R_S [Ω cm^2]	Calculated J_{SC} [mA/cm^2]
P3HT(Ref)	8.9	0.63	62.5	3.5	7.38	8.8
2-DO	13.8	0.63	56.1	4.9	5.28	13.4
3-DO	16.2	0.63	51.9	5.3	5.19	15.7
4-DO	14.3	0.63	56.6	5.1	5.30	13.9
6-DO	15.3	0.63	50.2	4.9	5.20	14.7
8-DO	10.9	0.63	53.2	3.1	5.56	10.4
10-DO	8.7	0.63	48.5	2.8	7.98	8.4

ITO(170 nm)/PEDOT:PSS(40 nm)/P3HT:PCBM:additive(130 nm)/BaF_2(2 nm)/Ba(2 nm)/Al(100 nm).

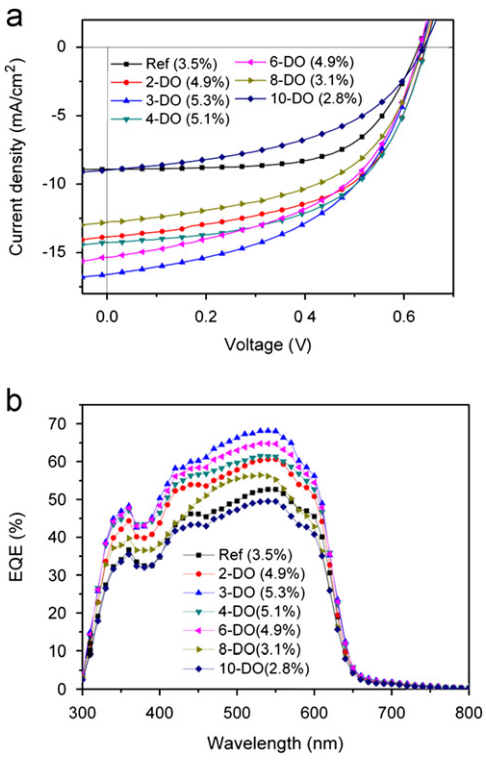

Fig. 2. (a) *J–V* characteristics and (b) external quantum efficiency (EQE) characteristics of P3HT:PCBM=1:0.6 composite films with alkanediol series as processing additives.

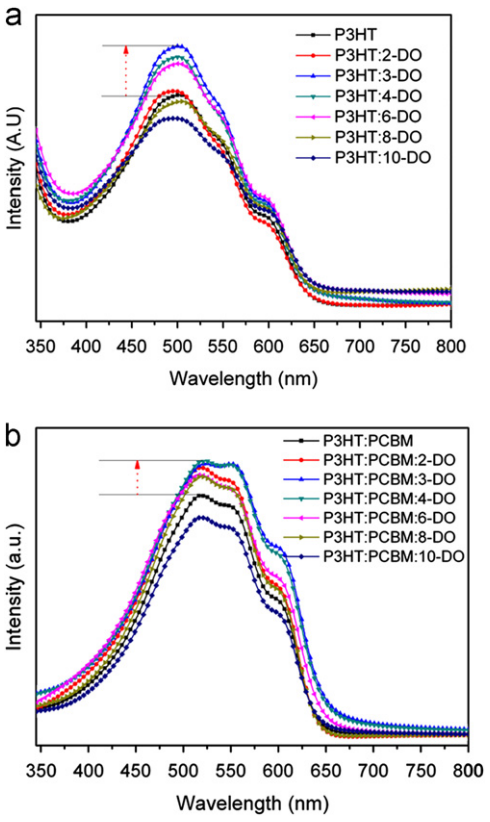

Fig. 3. UV–vis absorption spectra of (a) P3HT films with/without diol series and (b) P3HT:PCBM blending films with/without alkanediol series as processing additives.

P3HT–PCBM blended film as a processing additive. When 3-DO was added, in particular, an increase in absorbance over the wavelength range from 450 to 600 nm because of π–π transition among P3HT molecules was observed [32,35]. It contributes to the increase in the PCE compared to the device without processing additives. Because it can be estimated that crystallinity was improved compared to the P3HT:PCBM film to which processing additive was not added, X-ray diffraction (XRD) pattern was analyzed for confirmation.

To check ordering of P3HT chain by the addition of processing additive, XRD pattern was shown in Fig. 4. Increase in the intensity of (100) diffraction peak was observed at $2\theta = 4.9^{\circ}$ in the film to which alkanediol series was added, compared to the P3HT:PCBM blended film. In other words, an ordered lamellar structure with an interlayer spacing that originated from interdigitated alkyl chains of P3HT was observed in alkanediol series added films [36]. Moreover, increase in intensity means increase of crystallinity in P3HT. Therefore, alkanediol series (e.g.: 2-DO, 3-DO, 4-DO and 6-DO) had an impact on the phase separation of P3HT and PCBM; because fullerenes are selectively dissolved in alkanediol, three kinds of separate phases existed (Fig. S3): (1) a PCBM–alkanediol phase, (2) a P3HT aggregate phase, and (3) a P3HT–PCBM phase [32]. In addition, the alkanediol series has a higher boiling point than ODCB as a host solvent; PCBM tends to remain in mixture solution (during drying) longer than P3HT, thereby enabling control of the phase separation and the resulting morphology of the BHJ material [33,34]. As a result, the crystallinity of P3HT increased. Based on Scherrer's equation ($L = K\lambda / B\cos\theta$), the crystalline size of P3HT has been calculated. Whereas L is the average crystalline size of P3HT (100), B is the full width at half maximum (FWHM) of (100) peak, λ is the wavelength of the incident X-rays (0.154 nm), θ is the angle of refraction, and K is Scherrer's constant (0.9). Based on Scherrer's equation, the crystalline size of each P3HT was stated in Table 2. In P3HT to which no processing additive was added, crystalline size was about 21 nm. However, it gradually increased when 3-DO was added, with an increase of up to 25 nm. Increase of crystalline size in P3HT refers to improvement of mobility of a carrier which was created in the photoactive layer. As a result, J_{SC} of PSCs was dramatically improved. Therefore, PCE was improved as well. When 8-DO and 10-DO were added, however, the crystalline size rather slightly decreased to 20 and 19 nm, respectively, which indicates a decrease in the mobility of the carrier. Compared to the other processing additives, 8-DO and 10-DO had no selectively dissolving charateristics because they were dissolved in ODCB at 100 °C. Therefore, it appears that they could not control the phase separation and interrupted in P3HT from being crystallized Table 3.

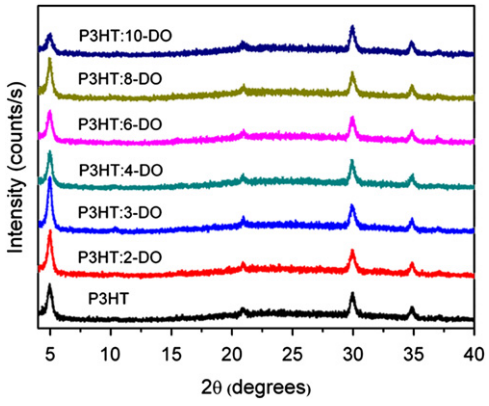

Fig. 4. X-ray diffraction pattern of P3HT:PCBM blend films with and without alkanediol series as processing additives.

After fabricating a hole-only device for a charge mobility study, the hole mobilities were calculated using the SCLC [37]. The configuration of hole-only devices was ITO/PEDOT:PSS/photoactive layer/MoO_3/Al. The reference device exhibited a hole mobility of 3.80×10^{-2} cm^2/Vs. The device in which 3-DO was doped to the photoactive layer had a hole mobility of 7.53×10^{-1} cm^2/Vs, which indicated that 3-DO improved carrier mobility. This result confirmed that doping with processing additives improved the photon-harvesting properties in the

Table 2
Crystalline size of P3HT.

Processing additives	Crystalline size of P3HT (nm)
None	21
2-DO	22
3-DO	25
4-DO	23
6-DO	22
8-DO	20
10-DO	19

Table 3
Boiling points and vapor pressures of solvent and various processing additives.

Solvent and processing additives	Boiling point (b.p./°C)
ODCB	180.5 °C
2-DO	197.3 °C
3-DO	211–217 °C
4-DO	235 °C
6-DO	208 °C (white solid)
8-DO	172 °C (white solid)
10-DO	297 °C (white solid)

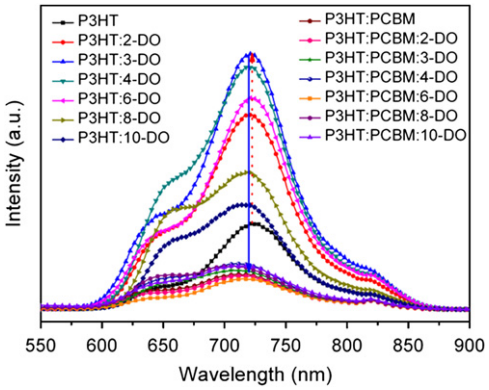

Fig. 5. PL quenching data of P3HT films with/without alkanediol series and P3HT:PCBM blend films with/without alkanediol series as processing additives.

Table 4
Calculated PL quenching area.

Processing additive	Quenching area (%)
None	47
2-DO	80
3-DO	82
4-DO	78
6-DO	78
8-DO	64
10-DO	50

photoactive layers and also enhanced hole mobility. Furthermore, processing additives were able to send the generated holes to the external circuit quickly without recombination.

Fig. 5 shows PL quenching in order to examine if the exciton which was generated on the photoactive layer has been efficiently dissociated. The difference between the area of the graph in which the acceptor PCBM was not included and the area of the graph in which it was included represents a quenched electron–hole. As the quenched amount increases, the efficiency of electron–hole dissociation improves. As shown in Table 4, 47%

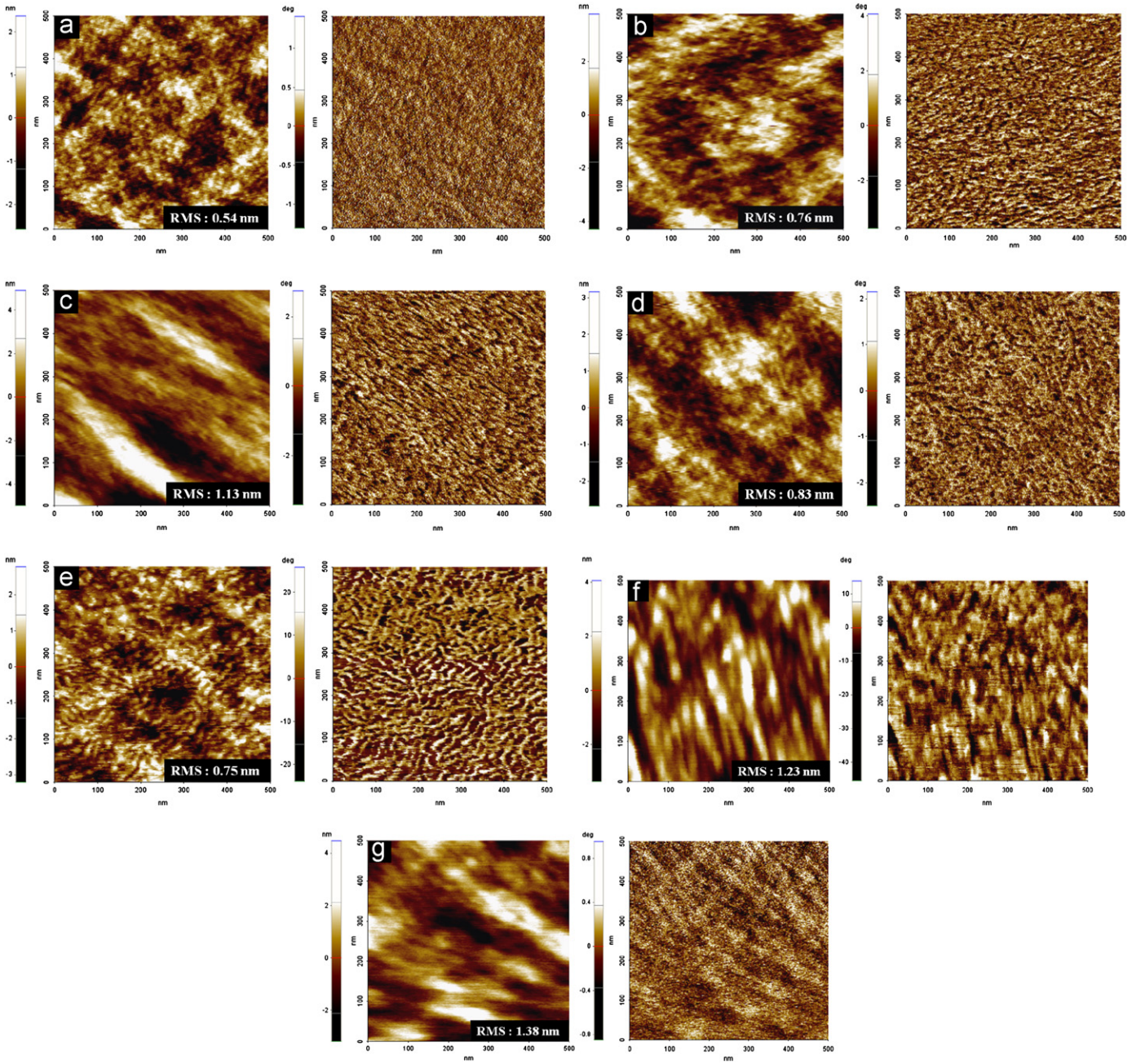

Fig. 6. Tapping-mode AFM images of films cast from P3HT:PCBM with/without alkanediol series as processing additives. The topology of each film is shown in the left panels, and corresponding phase images in the right panels. (a) P3HT:PCBM, (b) 2-DO, (c) 3-DO, (d) 4-DO, (e) 6-DO, (f) 8-DO and (g) 10-DO.

Table 5
Surface energy of P3HT and PCBM with various processing additives.

P3HT	P3HT	P3HT+2-DO	P3HT+3-DO	P3HT+4-DO	P3HT+6-DO	P3HT+8-DO	P3HT+10-DO
Surface energy [mJ/m^2]	19.13	18.92	19.43	18.76	18.88	20.78	22.72
PCBM	PCBM	PCBM+2-DO	PCBM+3-DO	PCBM+4-DO	PCBM+6-DO	PCBM+8-DO	PCBM+10-DO
Surface energy [mJ/m^2]	22.49	21.19	20.74	20.80	20.95	26.23	28.34

Host solvent: ODCB.

of quenching ratio was observed in P3HT in which processing additives were not added to the photoactive layer, and 82% of quenched ratio (increase by 74%) was detected when 3-DO was added. In fact, it was greater than P3HT in terms of quenched ratio. Therefore, the addition of processing additives improves absorption properties by causing π–π transition among P3HT molecules and promotes carrier mobility by increasing crystallinity in P3HT. Therefore, it is able to absorb more photons when processing additives are not added to make them quickly to transfer to the external circuit without causing them from being recombined. To find out what structural properties the processing additives would have on the BHJ-structured photoactive layer, they were analyzed through AFM and TEM.

Fig. 6 shows changes in surface morphology by addition/no addition and type of processing additive in the P3HT:PCBM films, which were observed through AFM. From the height images, the root mean square (RMS) roughness of P3HT:PCBM film without processing additive (0.54 nm) was lower than with added processing additives in P3HT:PCBM films (from 0.76 to 1.38 nm). The surface roughness indicates the ordering of polymer self-organization [27]. As shown in Fig. 6(b)–(e), the texture is rougher than that of un-treated film and PCBM cluster and valleys are observed. By comparing these results with the device performance, the rough surface is signature of high performance PSCs [27]. From the phase images, highly ordered fibrillar crystalline domains are clearly visible in Fig. 6(b)–(e). This suggests that highly ordered P3HT chain alignment is achieved when processing additives are added in the host solvent. However rough surface and highly ordered fibrillar crystalline domains may effectively reduce the charge-transport distance and increase the J_{SC}, and at the same time provide nano-scaled texture that further enhances internal light scattering and light absorption. Therefore, it has been confirmed that (b)–(e) were more effective than (a) in terms of donor–acceptor phase separation. Compared to (a), relatively more effective phase separation was observed in (c) to which 3-DO was added. The processing additive such as 3-DO melts PCBM only with selective solubility. In addition, because it has higher b.p. compared to ODCB, the ODCB dissolved donor 'P3HT' forms better polymer ordering during vacuum treatment. Then, PCBM-dissolved processing additive forms PCBM cluster. Moreover, the surface energy of P3HT changed with 3-DO. Table 5 shows the surface energies of P3HT and PCBM with various processing additives. Among the surface energies of P3HT with processing additives, 3-DO added P3HT (19.43 mJ/m^2) has similar surface energy as 3-DO added PCBM (20.74 mJ/m^2). Therefore, similar surface energies of these individual compounds result in homogeneous blend and well-mixed films, resulting from the optimal phase separation of the PCBM domain after vacuum treatment. With the addition of 3-DO, the nano-scale domain can provide a pathway through which hole and electron which were separated after forming an interpenetrating network can be transferred to the cathode, can increase J_{SC} and prevent them from being recombined while the carrier is on the move. Therefore, R_S decreased in the devices to which processing additives except for 8-DO and 10-DO were added. In (e) to which 8-DO and 10-DO were added, however, very large-size agglomerated PCBM or P3HT clusters were formed. With very rough RMS, it has been confirmed that the domains were aggregated. Because it failed to form a bicontinuous network, efficiency was decreased.

Fig. 7 shows TEM images of thin films in which 0.7 vol% of 3-DO was added to P3HT:PCBM and without addition of processing additive to P3HT:PCBM. Relatively dark regions in the TEM image indicate PCBM-rich regions or clusters because the P3HT (1.10 g/cm^3) has lower density compared to PCBM (1.50 g/cm^3) [24]. As shown in Fig. 6(b)–(e), P3HT:PCBM thin film to which processing additives were added was wider than P3HT:PCBM thin film (a) in which no additive was added in terms of dark area distribution. Though these images, we were able to determine that PCBM clusters formed. From the selected area electron diffraction (SAED) pattern in Fig. 7(b) inset, furthermore, improvement of crystallinity in P3HT was observed when 3-DO was added. Therefore, it was concluded that the control of morphology of the P3HT/PCBM blend and enhanced crystallinity of P3HT can be achieved through addition of processing additives, and separated hole and electron can be effectively dissociated through phase separation.

5. Conclusion

In summary, we have fabricated P3HT:PCBM based PSCs and dramatically improved their efficiency by adding alkanediol series as processing additives without any thermal annealing process. With the addition of processing additives, the degree of crystallinity of P3HT has improved. Moreover, interpenetrating network has made it possible for a carrier to quickly move to the external circuit. In addition, absorbance has improved with the increase in photon harvesting properties. As a result, PCE has improved by 52% due to the increase in J_{SC}.

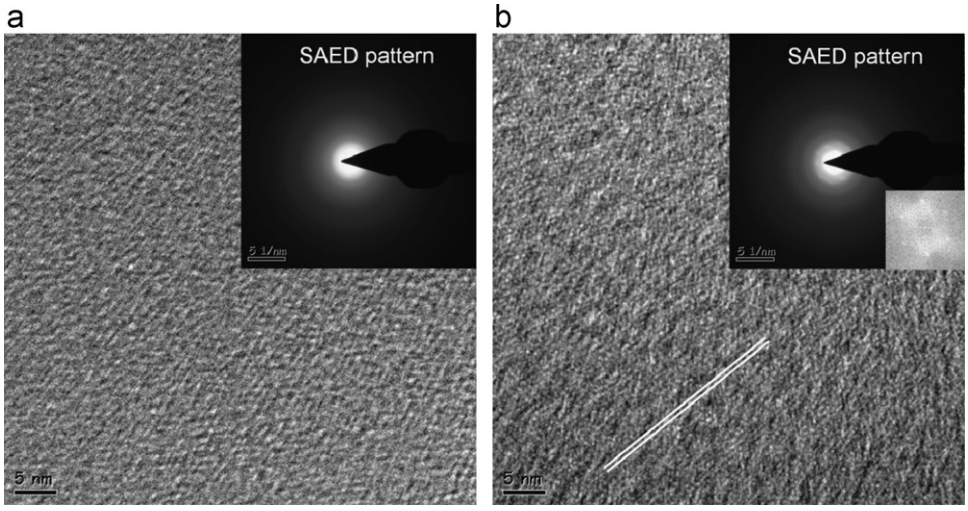

Fig. 7. TEM image of films cast from P3HT:PCBM (a) without processing additive (inset: SAED pattern) and (b) with 3-DO (inset: SAED pattern).

Appendix A. Supporting information

Supplementary data associated with this article can be found in the online version at http://dx.doi.org/10.1016/j.solmat.2013.02.004.

References

[1] L. Huang, M. Stolte, H. Bürckstümmer, F. Würthner, High-performance organic thin-film transistor based on a dipolar organic semiconductor, Advanced Materials 24 (2012) 5750–5754.
[2] P. Lin, F. Yan, Organic thin-film transistors for chemical and biological sensing, Advanced Materials 24 (2012) 34–51.
[3] H.J. Song, D.H. Kim, T.H. Lee, D.K. Moon, Emission color tuning of copolymers containing polyfluorene, benzothiadiazole, porphyrin derivatives, European Polymer Journals 48 (2012) 1485–1494.
[4] I.S. Song, S.W. Heo, J.H. Lee, J.R. Haw, D.K. Moon, Study on the wet processable antimony tin oxide (ATO) transparent electrode for PLEDs, Journal of Industrial and Engineering Chemistry 18 (2012) 312–316.
[5] I.S. Song, S.W. Heo, J.R. Ku, D.K. Moon, Study on the antimony tin oxide as a hole injection layer for polymer light emitting diodes, Thin Solid Films 520 (2012) 4068–4073.
[6] F.C. Krebs, Fabrication and processing of polymer solar cells: a review of printing and coating techniques, Solar Energy Materials and Solar Cells 93 (2009) 394–412.
[7] J. Alstrup, M. Jørgensen, A.J. Medford, F.C. Krebs, Ultra fast and parsimonious materials screening for polymer solar cells using differentially pumped slot-die coating, ACS Applied Materials and Interfaces 2 (2010) 2819–2827.
[8] E. Bundgaard, O. Hagemann, M. Manceau, M. Jørgensen, F.C. Krebs, Low band gap polymers for roll-to-roll coated polymer solar cells, Macromolecules 43 (2010) 8115–8120.
[9] M. Manceau, D. Angmo, M. Jørgensen, F.C. Krebs, ITO-free flexible polymer solar cells: from small model devices to roll-to-roll processed large modules, Organic Electronics 12 (2011) 566–574.
[10] F.C. Krebs, J. Fyenbob, M. Jørgensen, Product integration of compact roll-to-roll processed polymer solar cell modules: methods and manufacture using flexographic printing, slot-die coating and rotary screen printing, Journal of Materials Chemistry 20 (2010) 8994–9001.
[11] F.C. Krebs, Roll-to-roll processing and product integration of polymer solar cells, Energy and Environmental Science 3 (2010) 512–525.
[12] S.W. Heo, J.Y. Lee, H.J. Song, J.R. Ku, D.K. Moon, Patternable brush painting process for fabrication of flexible polymer solar cells, Solar Energy Materials and Solar Cells 95 (2011) 3041–3046.
[13] S.W. Heo, K.W. Song, M.H. Choi, T.H. Sung, D.K. Moon, Patternable solution process for fabrication of flexible polymer solar cells using PDMS, Solar Energy Materials and Solar Cells (2011) 3564–3572.
[14] G. Yu, J. Gao, J.C. Hummelen, F. Wudl, A.J. Heeger, Polymer photovoltaic cells: enhanced efficiencies via a network of internal donor–acceptor heterojunctions, Science 270 (1995) 1789–1791.
[15] H.Y. Chen, J.H. Hou, S.Q. Zhang, Y.Y. Liang, G.W. Yang, Y. Yang, L.P. Yu, Y. Wu, G. Li, Polymer solar cells with enhanced open-circuit voltage and efficiency, Nature Photonics 3 (2009) 649–653.
[16] P.W.M. Blom, V.D. Mihailetchi, L.J.A. Koster, D.E. Markov, Device physics of polymer: fullerene bulk heterojunction solar cells, Advanced Materials 19 (2007) 1551–1566.
[17] Y. Wang, L. Yang, C. Yao, W. Qin, S. Yin, F. Zhang, Enhanced performance and stability in polymer photovoltaic cells using lithium benzoate as cathode interfacial layer, Solar Energy Materials and Solar Cells 95 (2011) 1243–1247.
[18] J.M. Yun, J.S. Yeo, J. Kim, H.G. Jeong, D.Y. Kim, Y.J. Noh, S.S. Kim, B.C. Ku, S.I. Na, Solution-processable reduced graphene oxide as a novel alternative to PEDOT:PSS hole transport layers for highly efficient and stable polymer solar cells, Advanced Materials 23 (2011) 4923–4928.
[19] Z. He, C. Zhong, X. Huang, W.-Y. Wong, H. Wu, L. Chen, S. Su, Y. Cao, Simultaneous enhancement of open-circuit voltage, short-circuit current density, and fill factor in polymer solar cells, Advanced Materials 23 (2011) 4636–4643.
[20] Z. He, C. Zhong, S. Su, M. Xu, H. Wu, Y. Cao, Enhanced power-conversion efficiency in polymer solar cells using an inverted device structure, Nature Photonics 3 (2012) 649–653.
[21] P. Schilinsky, C. Waldauf, C.J. Brabec, Recombination and loss analysis in polythiophene based bulk heterojunction photodetectors, Applied Physics Letters 81 (2002) 3885–3887.
[22] F. Padinger, R.S. Rittberger, N.S. Sariciftci, Effects of postproduction treatment on plastic solar cells, Advanced Functional Materials 13 (2003) 85–88.
[23] M. Riedel, V. Dyakonov, Influence of electronic transport properties of polymer–fullerene blends on the performance of bulk heterojunction photovoltaic devices, Physica Status Solidi A 201 (2004) 1332–1341.
[24] X. Yang, J. Loos, S.C. Veenstra, W.J.H. Verhees, M.M. Wienk, J.M. Kroon, M.A.J. Michels, R.A.J. Janssen, Nanoscale morphology of high-performance polymer solar cells, Nano Letters 5 (2005) 579–583.
[25] Y. Kim, S.A. Choulis, J. Nelson, D.D.C. Bradley, S. Cook, J.R. Durrant, Device annealing effect in organic solar cells with blends of regioregular poly(3-hexylthiophene) and soluble fullerene, Applied Physics Letters 86 (2005) 063502-1–063502-3.
[26] G. Li, V. Shrotriya, Y. Yao, Y. Yang, Investigation of annealing effects and film thickness dependence of polymer solar cells based on poly(3-hexylthiophene), Journal of Applied Physics 94 (2005) 043704-1–043704-5.
[27] G. Li, V. Shrotriya, J. Huang, T. Mariarty, K. Emery, Y. Yang, High-efficiency solution processable polymer photovoltaic cells by self-organization of polymer blends, Nature Materials 4 (2005) 864–868.
[28] M. Reyes-Reyes, K. Kim, D.L. Carroll, High-efficiency photovoltaic devices based on annealed poly(3-hexylthiophene) and 1-(3-methoxycarbonyl)-propyl-1-phenyl-(6,6) C_{61} blends, Applied Physics Letters 87 (2005) 083506-1–083506-3.
[29] W. Ma, C. Yang, X. Gong, K. Lee, A.J. Heeger, Thermally stable, efficient polymer solar cells with nanoscale control of the interpenetrating network morphology, Advanced Functional Materials 15 (2005) 1617–1622.
[30] Y. Kim, S. Cook, S.M. Tuladhar, S.A. Choulis, J. Nelson, J.R. Durrant, D.D.C. Bradley, M. Giles, I. McCulloch, C.-S. Ha, M. Ree, A strong regioregularity effect in self-organizing conjugated polymer films and high-efficiency polythiophene:fullerene solar cells, Nature Materials 5 (2006) 197–203.
[31] F. Zhang, K.G. Jespersen, C. Bjorstrom, M. Svensson, M.R. Andersson, V. Sundstrom, K. Magnusson, E. Moons, A. Yartsev, O. Inganas, Influence of solvent mixing on the morphology and performance of solar cells based on polyfluorene copolymer/fullerene blends, Advanced Functional Materials 16 (2006) 667–674.
[32] J.K. Lee, W.L. Ma, C.J. Brabec, J. Yuen, J.S. Moon, J.Y. Kim, K. Lee, G.C. Bazan, A.J. Heeger, Processing additives for improved efficiency from bulk heterojunction solar cells, Journal of the American Chemical Society 130 (2008) 3619–3623.
[33] J. Peet, N.S. Cho, S.K. Lee, G.C. Bazan, Transition from solution to the solid state in polymer solar cells cast from mixed solvents, Macromolecules 41 (2008) 8655–8659.
[34] W. Wang, H.B. Wu, C.Y. Yang, C. Luo, Y. Zhang, J.W. Chen, Y. Cao, High-efficiency polymer photovoltaic devices from regioregular-poly(3-hexylthiophene-2,5-diyl) and [6,6]-phenyl-C_{61}-butyric acid methyl ester processed with oleic acid surfactant, Applied Physics Letters 90 (2007) 183512-1–183512-3.
[35] Y.-M. Chang, L. Wang, Efficient poly(3-hexylthiophene)-based bulk heterojunction solar cells fabricated by an annealing-free approach, The Journal of Physical Chemistry C 112 (2008) 17716–17720.
[36] P. Vanlaeke, A. Swinnen, I. Haeldermans, G. Vanhoyland, T. Aernouts, D. Cheyns, C. Deibel, J. D'Haen, P. Heremans, J. Poortmans, J.V. Manca, Solar Energy Materials and Solar Cells 90 (2006) 2150–2158.
[37] S.W. Heo, I.S. Song, Y.S. Kim, D.K. Moon, Fabrication of OPVs by introducing a conductivity-enhanced hybrid buffer layer, Solar Energy Materials and Solar Cells 101 (2012) 295–302.